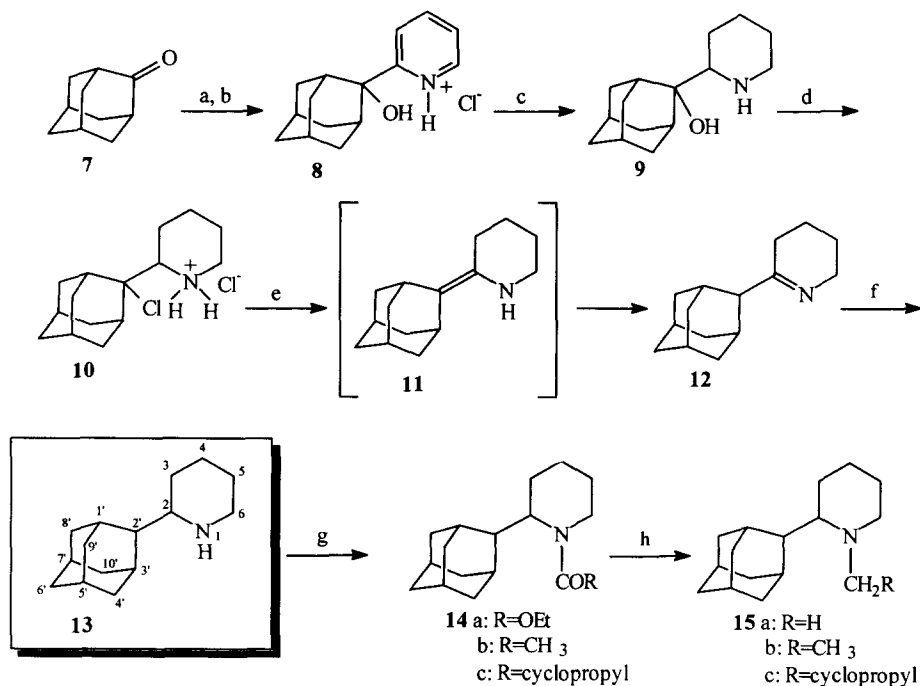


0960-894X/99/\$ - see front matter © 1999 Published by Elsevier Science Ltd. All rights reserved.
PII: S0960-894X(99)00631-9

The promising high activity of the synthetic compound **3** ($R=CH_3$) and the need for better tolerated drugs, prompted us to substitute the 2-position of adamantane with a piperidine heterocycle and investigate the *anti*-influenza virus activity relationships of the newly synthesized 2-(2-adamantyl)piperidines **13** and **15a-c**. 2-(2-adamantyl)piperidines **13** and **15a-c** are characterized by rigidity, except that the piperidine heterocycle can rotate with respect to the adamantane nucleus.

The synthetic route followed for the preparation of the novel compounds **13** and **15a-c** is illustrated in Scheme 1. Tertiary alcohol **8** was synthesized from adamantanone **7** and 2-pyridinyl lithium followed by treatment with HCl. The catalytic hydrogenation of the hydrochloride **8** over PtO_2 catalyst led to the aminoalcohol **9**. Reaction of alcohol **9** with $SOCl_2$ gave the corresponding chloride **10** as hydrochloride. Elimination reaction of chloride **10** in refluxing KOH/EtOH solution produced piperidine **12** possibly via the unstable enamine **11**. Imine **12** was treated with sodium borohydride to give the parent 2-(2-adamantyl)piperidine **13**.⁷ The latter was *N*-alkylated to the piperidines **15a-c** through $LiAlH_4$ reduction of compounds **14a-c**.⁷

Scheme 1



Reagents: (a) 2-pyridinyl lithium, Et_2O/THF , $-60^\circ C$ and then HCl 10% (82%); (b) gas HCl, EtOH; (c) H_2/PtO_2 , EtOH and then Na_2CO_3 10% (97%); (d) $SOCl_2$, CH_2Cl_2 , 6h reflux; (e) KOH, EtOH, RT for 24h under argon and then gentle reflux for 3h (61% from **9**); (f) $NaBH_4$, MeOH, $0-5^\circ C$ and then RT for 5h (94%); (g) $RCOCl$, Et_3N , Et_2O or THF, $0-5^\circ C$ and then RT for 24h (84-94%); (h) $LiAlH_4$, THF, 15h reflux (74-89%).

The cytotoxicity and activity of the new aminoadamantane heterocycles **13** and **15a–c** were examined against influenza A virus (strains H₂N₂ and H₃N₂) and influenza B virus according to previously reported methods (Table 1).⁸

Table 1 Anti-influenza virus activity and cytotoxicity of aminoadamantane derivatives **13**, **15a–c**^a in MDCK cells.^b

Compound	MIC ₅₀ ^c (μM)			MTC ₅₀ ^d (μM)
	Influenza virus A	Influenza virus A	Influenza virus B ^b	
	H ₂ N ₂ ^b	H ₃ N ₂ ^b		
13	7.8	≥977	>977	≥977
15a	>143	>143	>143	977
15b	>28	>28	>28	143
15c	143	>143	>143	977
Amantadine	28.3	-	-	1333
Rimantadine	20.9	≥56	≥93	1160
Ribavirin	31.1	41.0	41.0	>1025

^aAminoadamantanes **13** and **15a–c** were tested as hydrochlorides or fumarate salts. ^bAbbreviations and strains used: MDCK, Madin-Darby canine kidney; influenza A H₂N₂ (A2 Japan/305/57), influenza A H₃N₂ (X31), influenza B (Hong Kong/5/72). ^cMinimum inhibitory concentration required to reduce virus-induced cytopathicity by 50%.

^d Minimum cytotoxic concentration to reduce the viability of MDCK cells by 50%. All data represent mean values for at least two separate experiments.

From the MIC₅₀ and MTC₅₀ values presented in Table 1, it appears that compound **13** possesses 3–4 times higher activity against influenza A H₂N₂ virus strain than amantadine or rimantadine and a SI=125. H₂N₂ strain has an exquisite sensitivity to amantadine and rimantadine. Interestingly, no activity was exerted by the *N*-methylpiperidine **15a** or any of the other two *N*-substituted derivatives **15b–c**. This prompted us to explore the conformational properties of the novel synthetic compounds. This conformational analysis seeks for conformational differences and similarities between the active synthetic compound **13** and the almost inactive ones **15a–c**.

The combination of molecular dynamics simulation and grid scan search analysis for compounds **13** and **15a–c** resulted in the low-energy conformers **A–D** (Table 2).^{3,6,9,10} In Table 2 are shown the calculated conformational energies for the parent piperidine **13** and *N*-methylpiperidine **15a**. The C2–C2' bond conformation in all low energy conformers was found to be *anti*.

The most probable conformations **B** and **D** for compounds **13** and **15a** respectively resulting from computational chemistry are shown in Figure 2.

The obtained most probable conformer **B** of the parent piperidine **13** using computational analysis is supported by ^1H -NMR spectroscopy. The peak at 2.68 ppm assigned to H-2 appear as a triplet ($J \approx 10$ Hz). This proves its axial position and its *anti*-orientation relative to H-2'.

Table 2. Low energy conformers of piperidine **13** and *N*-methylpiperidine **15a**. Energies were calculated using the MM2 force field.¹¹

Compound	Conformer	Conformer descriptors		Energy (kcal·mol ⁻¹)
		<i>N</i> -R orientation	Adamantane orientation	
13	A	equatorial	equatorial	27.3
	B	axial	equatorial	26.8
	C	equatorial	axial	29.1
	D	axial	axial	29.0
15a	A	equatorial	equatorial	37.2
	B	axial	equatorial	33.8
	C	equatorial	axial	37.5
	D	axial	axial	34.4

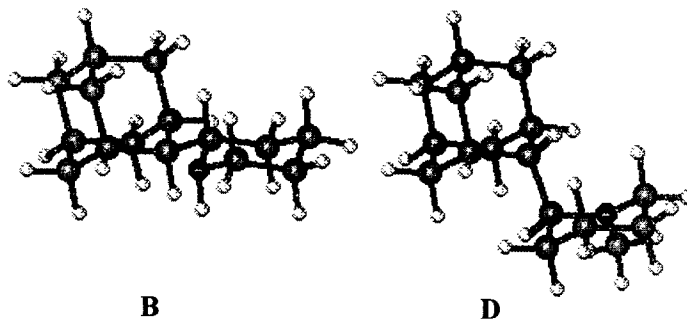


Figure 2 Low energy conformations of compounds **13** and **15a** resulting from computational chemistry.

The dynamics analysis results show that conformation **D** in which adamantane and *N*-alkyl substituent have an axial orientation is the most probable one for *N*-alkylpiperidines. The two piperidine substituents in conformer **D** adopt axial positions in order to avoid their energy-consuming steric interactions. ^{13}C -NMR spectroscopy results provide evidence for the low energy conformation **D**. For example, in derivative **15a** the resonances at (25.1, 19.3, 20.4 ppm), attributed to carbons 3, 4 and 5 respectively, were shifted 6–7 ppm upfield with respect to the corresponding resonances of the parent *N*-H heterocycle **13** (at 30.8, 25.3, 27.0 ppm) because of the γ -gauche effect exerted by the axial *N*-CH₃ and adamantane groups. The ^{13}C chemical shift at 35.1 ppm, attributed to the *N*-methyl group, confirms its axial orientation.^{3,6,9}

The conformers **B** and **D** for piperidines **13** and **15a** resulting from a combination of NMR spectroscopy and computational chemistry analysis were superimposed in order to reveal the similarities and differences in structure (Figure 3). The strategy of overlay fit was to match adamantane rings and examine any spatial differences between the atoms of the two piperidine heterocycles. The results show that atoms of the two piperidine heterocycles occupy different spatial position (3.1 Å apart).

The conformational change depicted in *N*-alkyl piperidines may contribute to the dramatic decrease of the activity in *N*-alkyl piperidines **15a-c** against H₂N₂ influenza virus A. Such a conformational-activity change between the parent and *N*-alkyl derivatives was not observed for aminoadamantanes **3-6**.^{5,6}

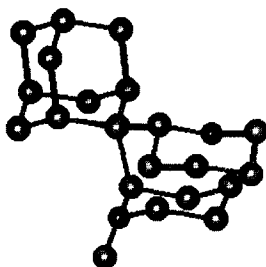


Figure 3 Superposition of low energy conformers **B** and **D** of piperidines **13** and **15a** respectively.

To our knowledge the dramatic loss of activity upon *N*-methylation in aminoadamantanes has never been observed in any other series studied. The new compounds did not exhibit any activity against influenza A H₃N₂ virus and influenza B virus. These observations indicate that there are certain stereoelectronic relationships between adamantane and amino pharmacophore groups to allow aminoadamantanes to exert their M2 ion channel blocking activity.¹⁻³

Studies using dynamic NMR spectroscopy and simulation analysis are currently underway to describe in detail the conformational characteristics of 2-(2-adamantyl)-piperidines.⁶ The effect of *N*-dialkylaminoethyl substitution will be also explored as some *N*-dialkylaminoethyl substituted 2-(1-adamantyl)piperidines exhibit promising anti-HIV-1 activity.¹²

Acknowledgment: This research activity was supported by a research grant from the University of Athens, Greece.

References and Notes

- (a) Hay, A. J.; Wolstenholme, A. J.; Skehel, J. J.; Smith, M. H. *EMBO J.* **1985**, *4*, 3021-3024. (b) Hay, A. J. *Semin. Virol.* **1992**, *3*, 21-30. (c) Pinto, L. H.; Holsinger, L. J.; Lamb, R. A. *Cell* **1992**, *69*, 517-528. (d) Duff, K. C.; Gilchrist, P. J.; Saxena, A. M.; Bradshaw, J. P. *Virology* **1992**, *188*, 14-24.
- In *Burger's Medicinal Chemistry and Drug Discovery: Therapeutic Agents*; Wolff, M. E., Ed.; John Wiley & Sons: New York, 5th Ed. (1997); Vol. 4; pp 590-591.

3. Kolocouris, A. Ph.D Thesis (1995).
4. Kolocouris, N.; Foscolos, G. B.; Kolocouris A.; Marakos, P.; Pouli, N.; Fytas, G.; Ikeda, S.; De Clercq, E. *J. Med. Chem.* **1994**, *37*, 2896-2902.
5. Kolocouris, N.; Kolocouris A.; Foscolos G. B.; Fytas, G.; Neyts, J.; Padalko, E.; Balzarini, J.; Snoeck, R.; Andrei, G.; De Clercq, E. *J. Med. Chem.* **1996**, *39*, 3307-3318.
6. Kolocouris, A.; Micros, E.; Kolocouris, N. *J. Chem. Soc. Perkin. Trans. 2* **1998**, 1701-1708.
7. The ^1H and ^{13}C NMR spectra of piperidine **13** were assigned using COSY, CHCORR and NOESY spectroscopy. ^1H NMR (CDCl_3 , 300 MHz): δ 0.86-1.0 (m, 1H, 3ax-H), 1.22-2.0 (m, 20H, 1',2',4',5',6',7',8',9',10'-H, N-H, 3eq, 4, 5-H), 1.95 (bs, 1H, 3'-H), 2.55-2.75 (m, 2H, 2, 6ax-H), 3.04-3.13 (m, 1H, 6eq-H); ^{13}C NMR (CDCl_3 , 75 MHz) δ 25.3 (4-C), 27.0 (5-C), 28.0, 28.1, 28.3, 28.7 (7',5',3',1'-C), 30.8 (3-C), 32.2, 32.5 (4',9'-C), 38.4 (6'-C), 39.1, 39.5 (8',10'-C), 47.7 (6-C), 49.9 (2'-C), 56.0 (2-C).
Spectra and elemental analysis of all the synthesized compounds were in accord with their structure.
8. Shigeta, S.; Konno, K.; Yokota, T.; Nakamura, K.; De Clercq, E. *Antimicrob. Agents Chemother.* **1998**, *32*, 906-911.
9. (a) Crabb, T. A.; Katritzky, A. R. *Adv. Heter. Chem.* **1984**, *36*, 1-172. (b) Lambert J. B.; Takeuchi Y., in *Cyclic Organonitrogen Stereodynamics*, VCH, New York, 1992.
10. Molecular dynamics simulations were performed on a Silicon Graphics O2 station using QUANTA software package and CHARMM force field. Thus, an initial structure was constructed and minimized using conjugate gradient and Newton-Raphson algorithms and an energy gradient tolerance of $0.01 \text{ kcal}\cdot\text{mol}^{-1}\cdot\text{\AA}^{-1}$. The local minimum obtained was structure **C**. This structure was then subjected to dynamic simulation. The simulation study was carried out at 1000.0 K with time steps of 1 fs for 300 ps using an output frequency of 1 ps to sample 300 frames of conformers. The low energy structures **A-D** found were further analyzed by one bond grid scan searches using intervals of 5° . In each grid scan analysis three local minima were found corresponding to *anti*, g^+ and g^- orientation around C2-C2' bond. Conformers **A-D** with an *anti* orientation around C2-C2' bond were found to have the lowest energy content. For further details see: Mavromoustakos, T.; Kolocouris, A.; Zervou, M.; Roumelioti, P.; Matsoukas, J. M.; Weisemann, R. *J. Med. Chem.* **1999**, *42*, 1714-1722.
11. Calculations of the relative energies of conformations **A-D** were performed using MM2 calculations. These calculations give the most consistent results with experimental data for six-membered nitrogen heterocycles as described by Profeta, S.; Allinger, N. L. *J. Am. Chem. Soc.* **1985**, *107*, 1907-1918. The MM+ force field provided by the Hyperchem was used. This force field is an extension of MM2 force field.
12. Fytas, G.; Stamatiou, G.; Foscolos, G. B.; Kolocouris, A.; Kolocouris, N.; Witvrouw, M.; Pannecouque, C.; De Clercq, E. *Bioorg. Med. Chem. Lett.*, **1997**, 1887-1890.